Inorg. Chem. **2009**, *48*, 2391−2398

Anion Binding by Protonated Forms of the Tripodal Ligand Tren

Carla Bazzicalupi, Andrea Bencini, Antonio Bianchi,* Andrea Danesi, Claudia Giorgi, and Barbara Valtancoli

Department of Chemistry, University of Florence, Via della Lastruccia 3, 50019 Sesto Fiorentino, Italy

Received July 15, 2008

The interaction of the protonated forms of tris(2-aminoethyl)amine (tren) with NO_3^-, SO_4^{2-}, TsO^-, PO_4^{3-}, $P_2O_7^{4-}$, and $P_3O_{10}^{5-}$ was studied by means of potentiometric and microcalorimetric measurements in a 0.10 M NMe_4Cl aqueous solution at 298.1 ± 0.1 K, affording stability constants and the relevant energetic terms $\Delta H°$ and $T\Delta S°$ of complexation. Thermodynamic data show that these anion complexation processes are mainly controlled by electrostatic forces, although hydrogen-bond interactions and solvation effects also contribute to complex stability, leading, in some cases, to special $\Delta H°$ and $T\Delta S°$ contributions. The crystal structures of $[H_3L][NO_3]_3$ and $[H_3L][TsO]_3$ evidence a preferred tridentate coordination mode of the triprotonated ligands in the solid state. Accordingly, the H_3L^{3+} receptor binds a single oxygen atom of both NO_3^- and TsO^- by means of its three protonated fingers, although in the crystal structure of $[H_3L][TsO]_3$, one conformer displaying bidentate coordination was also found. Modeling studies performed on the $[H_3L(NO_3)]^{2+}$ complex suggested that the tridentate binding mode is the preferred one in aqueous solution, while in the gas phase, a different complex conformation in which the receptor interacts with all three oxygen atoms of NO_3^- is more stable.

Introduction

The discovery by Park and Simmons[1] in 1968 that the macrobicyclic diamine ligands katapinand, in their protonated forms, could encapsulate halide anions heralded the origin of "anion coordination chemistry", but only few years later, the horizons of this new area of supramolecular chemistry were opened by Lehn and co-workers,[2] who understood the potentialities lying behind the supramolecular chemistry of anions and began to develop targeted anion receptors based on polyammonium macrocycles. Successively, an increasing number of anion receptors, many of which were of the polyammonium type and featured by a variety of molecular structures, were developed by different groups.[3]

The objective of achieving strong and selective anion binding is a challenging task, since anions generally have large size and variable shape, are strongly solvated, may only exist in specific media, and interact with receptors only through weak forces. Nevertheless, this objective has been successfully addressed by the synthesis of tailored receptors.[3−6] The most effective way to bind anions consists in taking advantage of their negative charge, and accordingly, polyammonium (positively charged) ligands, in particular protonated polyamines, have been the principal receptors of choice, since they ensure an adequate electrostatic attraction reinforced by hydrogen-bond contacts with the coordinated anions.[3−6] Three-dimensional polyamines, both cagelike and tripodal, have shown to be particularly useful in this respect, thanks to their preorganized architectures, which give rise to anion encryption at a low energetic cost for ligand conformation and with high energetic benefit from multiple

* To whom correspondence should be addressed. E-mail: antonio.bianchi@unifi.it.

(1) Park, C. H.; Simmons, H. E. *J. Am. Chem. Soc.* **1968**, *90*, 2431–2433.
(2) (a) Graf, E.; Lehn, J.-M. *J. Am. Chem. Soc.* **1976**, *98*, 6403–6405. (b) Lehn, J.-M.; Sonveaux, E.; Willard, A. K. *J. Am. Chem. Soc.* **1978**, *100*, 4914–4916.
(3) (a) Sessler, J. L.; Gale, P. A.; Cho, W. S. *Anion Receptor Chemistry (Monographs in Supramolecular Chemistry)*; Stoddart, J. F., Ed.; RSC: Cambridge, U. K., 2006. (b) *Supramolecular Chemistry of Anions*; Bianchi, A., Bowman-James, K., Garcia-España, E., Eds.; Wiley-VCH: New York, 1997.
(4) Schneider, H.-J.; Yatsimirsky, A. K. *Chem. Soc. Rev.* **2007**, *37*, 263–277.
(5) Garcia-España, E.; Díaz, P.; Llinares, J. M.; Bianchi, A. *Coord. Chem. Rev.* **2006**, *250*, 2952–2986.
(6) (a) Kang, S. O.; Hossain, Md. A.; Bowman-James, K. *Coord. Chem. Rev.* **2006**, *250*, 3038–3052. (b) Bowman-James, K. *Acc. Chem. Res.* **2005**, *38*, 671–678. (c) Llinares, J. M.; Powell, D.; Bowman-James, K. *Coord. Chem. Rev.* **2003**, *240*, 57–75. (d) McKee, V.; Nelson, J.; Town, R. M. *Chem. Soc. Rev.* **2003**, *32*, 309–325.

10.1021/ic8013128 CCC: $40.75
Published on Web 02/10/2009

host−guest interactions.[2,4−15] For instance, polyprotonated azacryptands bind anions, even monoanions, more strongly than their monocyclic analogues by two or more orders of magnitudes.[6c]

Since the beginning of anion coordination chemistry, the synthesis of three-dimensional receptors has been widely based on the use of the triamine tris(2-aminoethyl)amine (tren).[2b,4−15]

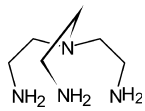

Due to the tripodal structure of tren, synthetic procedures involving this molecule spontaneously proceed toward the formation of receptors with cavities conformed in such a way as to promote anion encryption. In addition to such synthetic advantage, the use of this building block with C_3 symmetry promotes topological matching with anions of the same symmetry, among which there are oxoanions, a class of anions of great biological relevance and environmental concern.

(7) (a) Dietrich, B.; Guilhem, J.; Lehn, J.-M.; Pascard, C.; Sonveaux, E. *Helv. Chim. Acta* **1984**, *67*, 91–104. (b) Hosseini, M. W.; Lehn, J.-M. *Helv. Chim. Acta* **1988**, *71*, 749–756. (c) Dietrich, B.; Hosseini, M. W.; Lehn, J.-M.; Session, R. B. *Helv. Chim. Acta* **1985**, *68*, 289–299. (d) Heyer, D.; Lehn, J.-M. *Tetrahedron Lett.* **1986**, *27*, 5869–5872. (e) Fujita, T.; Lehn, J.-M. *Tetrahedron Lett.* **1988**, *29*, 1709–1712. (f) Lehn, J.-M.; Méric, R.; Vigneron, J.-P.; Bkouche-Waksman, I.; Pascard, C. *J. Chem. Soc., Chem. Commun.* **1991**, 62–64.

(8) (a) Hossain, Md. A.; Liljegren, J. A.; Powell, D.; Bowman-James, K. *Inorg. Chem.* **2004**, *43*, 3751–3755. (b) Kang, S. O.; Llinares, J. M.; Powell, D.; VanderVelde, D.; Bowman-James, K. *J. Am. Chem. Soc.* **2003**, *125*, 10152–10153. (c) Clifford, T.; Dandy, A.; Llinares, J. M.; Mason, S.; Alcock, N. W.; Powell, D.; Aguilar, J. A.; Garcia-España, E.; Bowman-James, K. *Inorg. Chem.* **2001**, *40*, 4710–4720. (d) Danby, A.; Seib, L.; Alcock, N. W.; Bowman-James, K. *Chem. Commun.* **2000**, 973–974. (e) Mason, S.; Clifford, T.; Seib, L.; Kuczera, K.; Bowman-James, K. *J. Am. Chem. Soc.* **1998**, *120*, 8899–8900.

(9) (a) Derossi, S.; Farrell, D. T.; Harding, C. J.; McKee, V.; Nelson, J. *Dalton Trans.* **2007**, 1762–1772. (b) Derossi, S.; Bond, A. D.; McKenzie, C. J.; Nelson, J. *Acta Crystallogr., Sect. E* **2005**, m1379–m1382. (c) Nelson, J.; Nieuwenhuyzen, M.; Pál, I.; Town, R. M. *Dalton Trans.* **2004**, 229–235. (d) Nelson, J.; Nieuwenhuyzen, M.; Pál, I.; Town, R. M. *Dalton Trans.* **2004**, 2303–2308. (e) Farrell, D.; Gloe, K.; Goretzki, G.; McKee, V.; Nelson, J.; Nieuwenhuyzen, M.; Pál, I.; Stephan, H.; Town, R. M.; Wichmann, K. *Dalton Trans.* **2003**, 1961–1968. (f) Hynes, M. J.; Maubert, B.; McKee, V.; Town, R. M.; Nelson, J. *J. Chem. Soc., Dalton Trans.* **2000**, 2853–2859.

(10) (a) Bazzicalupi, C.; Bencini, A.; Bianchi, A.; Danesi, A.; Giorgi, C.; Martinez Lorente, M. A.; Valtancoli, B. *New J. Chem.* **2006**, *30*, 959–965. (b) Bazzicalupi, C.; Bencini, A.; Bianchi, A.; Borsari, L.; Giorgi, C.; Valtancoli, B. *J. Org. Chem.* **2005**, *70*, 4257–4266. (c) Bazzicalupi, C.; Bencini, A.; Berni, E.; Bianchi, A.; Ciattini, S.; Giorgi, C.; Maoggi, S.; Paoletti, P.; Valtancoli, B. *J. Org. Chem.* **2002**, *67*, 9107–9110. (d) Bencini, A.; Bianchi, A.; Brazzini, S.; Fusi, V.; Giorgi, C.; Paoletti, P.; Valtancoli, B. *Inorg. Chim. Acta* **1998**, *273*, 326–333.

(11) (a) Beer, P. D.; Chen, Z.; Goulden, A. J.; Graydon, A.; Stokes, S. E.; Wear, T. *J. Chem. Soc., Chem. Commun.* **1993**, 1834–1836. (b) Beer, P. D.; Hopkins, P. K.; McKinney, J. D. *Chem. Commun.* **1999**, 1253–1254.

(12) Valiyaveettil, S. K.; Engbersen, J. F. J.; Verboom, W.; Reinhoudt, D. N. *Angew. Chem., Int. Ed. Engl.* **1993**, *32*, 900–901.

(13) Kavallieratos, K.; Danby, A.; Van Berkel, G. J.; Kelly, M. A.; Sachleben, R. A.; Moyer, B. A. *Anal. Chem.* **2000**, *72*, 5258–5264.

(14) Raposo, C.; Almaraz, M.; Martín, M.; Weinrich, V.; Mussóns, M. L.; Alcázar, V.; Caballero, M. C.; Morán, J. R. *Chem. Lett.* **1995**, 759–760.

(15) Ilioudis, C. A.; Tocher, D. A.; Steed, J. W. *J. Am. Chem. Soc.* **2004**, *126*, 12395–12402.

(16) Altomare, A.; Burla, M. C.; Cavalli, M.; Cascarano, G. L.; Giacovazzo, C.; Gagliardi, A.; Moliterni, A. G. G.; Polidori, G.; Spagna, R. *J. Appl. Crystallogr.* **1999**, *32*, 115–119.

Table 1. Crystal Data and Structure Refinement for $[H_3L][NO_3]_3$ and $[H_3L][TsO]_3$

	$[H_3L][NO_3]_3$	$[H_3L][TsO]_3$
empirical formula	$C_6H_{21}N_7O_9$	$C_{27}H_{42}N_4O_9S_6$
fw	335.30	759.005
wavelength (Å)	0.71069	1.54180
temp	room	room
collecting equipment	Enraf-Nonius CAD4	Brucker CCD
space group	$P2_1/n$	$P\bar{1}$
a (Å)	8.778(3)	11.830(1)
b (Å)	12.089(9)	16.831(2)
c (Å)	14.546(9)	17.681(2)
α (deg)	90.00	69.42(1)
β (deg)	90.78(4)	88.21(1)
γ (deg)	90.00	86.425(9)
volume (Å^3)	1543(2)	3289.2(6)
Za	4	2
Zb		2
D_{calcd} (mg/cm^3)	1.443	1.533
μ (mm^{-1})	0.133	4.342
R indices $[I > 2\sigma(I)]^a$	R1 = 0.0622	R1 = 0.1094
	wR2 = 0.1745	wR2 = 0.2881
R indices [all data]^a	R1 = 0.0848	R1 = 0.1450
	wR2 = 0.1974	wR2 = 0.3025

^{a} $R1 = \sum ||F_o| - |F_c|| / \sum |F_o|$; $wR2 = [\sum w(F_o^2 - F_c^2)^2 / \sum wF_o^4]^{1/2}$.

In spite of the center stage occupied by tren in the chemistry of anion receptors, its anion binding properties are, surprisingly, still undiscovered, although several simple tren derivatives have been prepared and studied,[8a,10c,11−15] including a recent tribenzylated tren molecule (tris(2-benzylaminoethyl)amine),[8a] which is a well-suited acyclic reference, in nonaqueous solvents, for tren-based macrobicycles containing benzene spacers.

To fill this gap, we performed a thermodynamic and structural study on the formation of NO_3^-, SO_4^{2-}, TsO^- (*p*-toluenesulfonate), PO_4^{3-}, $P_2O_7^{4-}$, and $P_3O_{10}^{5-}$ complexes with protonated forms of tren (L), including speciation of the complexes formed in aqueous solution, determination of stability constants and relevant energetic terms, $\Delta H°$ and $T\Delta S°$, of complexation, and the crystal structures of NO_3^- and TsO^- anions bound to the H_3L^{3+} receptor. Herein, we report the results of this study.

Experimental Section

Materials. The tren was purchased from Merck and purified as L·3HCl. High-purity $NaNO_3$, $Na_2HPO_4 \cdot 2H_2O$, $Na_4P_2O_7 \cdot 10H_2O$, $Na_5P_3O_{10} \cdot 6H_2O$, Na_2SO_4, and NaTsO employed in thermodynamic measurements and in the preparation of the crystalline adducts were purchased from Merck.

Crystals of $[H_3L][NO_3]_3$ and $[H_3L][TsO]_3$ suitable for X-ray analysis were prepared by the slow evaporation of aqueous solutions containing L and HNO_3 in a 1:4 molar ratio and, respectively, L and $TsOH \cdot H_2O$ in a 1:4 molar ratio.

X-Ray Crystallography. Single crystals of $[H_3L][NO_3]_3$ (**1**) and $[H_3L][TsO]_3$ (**2**) were analyzed by means of X-ray crystallography at room temperature. A summary of the resulting crystallographic data is reported in Table 1. The intensities of some reflections were monitored during data collection to check the stability of the crystals: no loss of intensity was observed. The integrated intensities were corrected for Lorentz and polarization effects. Both structures were solved by direct methods (SIR97).[16] Refinement was performed by means of full-matrix least-squares using the SHELX-

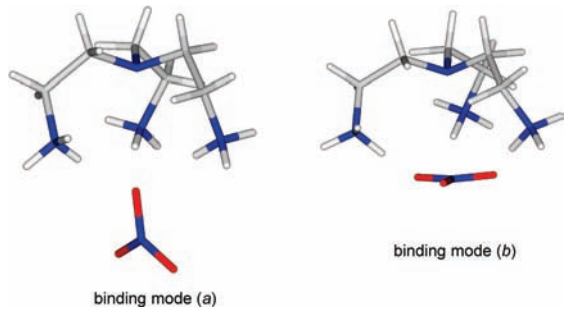

Figure 1. Conformations of $[H_3L(NO_3)]^{2+}$ used in molecular modeling calculations.

97 program.[17] In both structures, all non-hydrogen atoms were anisotropically refined.

In the case of **1**, an empirical absorption correction was applied. The hydrogen atoms linked to carbon atoms were introduced into calculated positions, and the thermal parameter was refined according to those of the linked atoms. The acidic protons were found in the ΔF map at the end of refinement, introduced into the calculation, and isotropically refined. The agreement factors at the end of refinement were R1 = 0.0622 for 237 refined parameters and 1896 observed reflections with $I > 2\sigma(I)$ and wR2 = 0.1974 for all data.

In the case of **2**, data acquisition, integration, reduction, and absorption correction were performed by using the SMART, SAINT, and SADABS programs.[18] Due to the high number of low-intensity reflections at high ϑ values, reflections with a sin ϑ/λ higher than 0.53 (d = 0.95 Å) were not used during refinement. The hydrogen atoms were introduced into calculated positions and isotropically refined using an overall fixed U = 0.05 Å^2.

Two crystallographically independent H_3L^{3+} cations and six *p*-toluenesulfonyl anions were found in the asymmetric unit. A high degree of disorder generally affected the *p*-toluenesulfonyl anions, while double positions were found for some ethylenic chains of the cations (N6, C51, C56, and C59 and N6′, C51′, C56′, and C59′ refined with population parameters of 0.6 and 0.4, respectively).

The agreement factors at the end of refinement were R1 = 0.0622 for 822 refined parameters and 4462 observed reflections with $I > 2\sigma(I)$ and wR2 = 0.3025 for all data.

Molecular Modeling. Quantum-mechanics calculations (DFT/B3LYP, 6-31G**, Jaguar v.6.0)[19] were carried out on two conformations of the $[H_3L(NO_3)]^{2+}$ anion adduct, considering the interaction of the three protonated primary amine groups of H_3L^{3+} with a single oxygen atom of NO_3^- (binding mode *a*), or with all three oxygen atoms (binding mode *b*), according to the schematic representations reported in Figure 1. Starting coordinates for binding mode *a* were obtained from the X-ray crystal structures of $[H_3L][NO_3]_3$ here reported, while appropriately modified coordinates taken from the crystal structure of a caged NO_3^- adduct[8e] were used for binding mode *b*. Solvent effects were taken into account by using the Poisson−Boltzmann solver.[20]

Molecular mechanics calculations were performed by means of the empirical force field method (AMBER3),[21] as implemented in HyperChem v.7.5.[22] Atomic charges were calculated at a semiempirical level of theory (PM3).[23] The TIP3P model was used for water molecules.[24] The solvent box was defined as a "cube" of 12 Å length, containing 34 water molecules. Conjugate gradient minimizations (2000 cycles, energy gradient < 0.001 kcal/mol) were performed after one cycle of the simulated annealing procedure (T = 300 K, equilibration time = 3 ps, run time = 3 ps, cooling time = 3 ps, and time step = 1.0 fs).

Potentiometric Measurements. All pH-metric measurements (pH = −log [H$^+$]) employed for the determination of equilibrium constants were carried out in 0.10 M NMe_4Cl solutions at 298.1 ± 0.1 K, using equipment and a methodology that has been already described.[25] The combined Hamilton electrode (LIQ-GLASS 238000/08) was calibrated as a hydrogen concentration probe by titrating known amounts of HCl with CO_2-free NaOH solutions and determining the equivalent point by Gran's method,[26] which allows one to determine the standard potential $E°$ and the ionic product of water (pK_w = 13.83(1) at 298.1 ± 0.1 K in 0.10 M NMe_4Cl). At least three measurements (about 100 data points for each one) were performed for each system in the pH range 2.5−10.5. In all experiments, the ligand concentration [L] was about 1×10^{-3} M. In the anion binding experiments, the anion concentration was varied in the range [L] ≤ [anion] ≤ 2[L]. The computer program HYPERQUAD[27] was used to calculate the equilibrium constants from emf data. Protonation constants of tren and anions were redetermined under our experimental conditions (Table S1, Supporting Information).

Microcalorimetric Measurements. The enthalpies of ligand protonation and anion binding were determined in a 0.10 M NMe_4Cl solution by means of an automated system composed of a Thermometric AB thermal activity monitor (model 2277) equipped with a perfusion-titration device and a Hamilton Pump (model Microlab M) coupled with a 0.250 cm^3 gastight Hamilton syringe (model 1750 LT). The microcalorimeter was checked by determining the enthalpy of reaction of a strong base (NMe_4OH) with strong acid (HCl) solutions. The value obtained (−56.7(2) kJ/mol) was in agreement with the literature values.[28] Further checks were performed by determining the enthalpies of protonation of ethylenediamine.

In a typical experiment, a NMe_4OH solution (0.10 M, addition volumes 15 μL) was added to acidic solutions of the ligands (5×10^{-3} M, 1.5 cm^3), containing equimolar quantities of the anion in the binding experiments. Corrections for heats of dilution were applied. The corresponding enthalpies of reaction were determined from the calorimetric data by means of the AAAL program.[29]

The enthalpy changes for ligand and anion protonation were redetermined under our experimental conditions (Table S1, Supporting Information).

(17) Sheldrick, G. M. *SHELXL-97*; University of Göttingen: Göttingen, Germany, 1997.
(18) *Brucker Molecular Analysis Research Tool*, v. 5.625; Brucker AXS: Madison, WI, 1997−2000.
(19) *Jaguar*, version 6.0; Schrödinger, LLC: New York, 2005.
(20) (a) Tannor, D. J.; Marten, B.; Murphy, R.; Friesner, R. A.; Sitkoff, D.; Nicholls, A.; Ringnalda, M.; Goddard, W. A., III.; Honig, B. *J. Am. Chem. Soc.* **1994**, *116*, 11875–11882. (b) Marten, B.; Kim, K.; Cortis, C.; Friesner, R. A.; Murphy, R. B.; Ringnalda, M. N.; Sitkoff, D.; Honig, B. *J. Phys. Chem.* **1996**, *100*, 11775–11778.
(21) Weiner, S. J.; Kollman, P. A.; Nguyen, D. T.; Case, D. A. *J. Comput. Chem.* **1986**, *7*, 230–252.
(22) *Hyperchem β1*, release 7.51 for Windows MM System; Hypercube, Inc.: Gainesville, FL.
(23) Steward, J. P. P. *J. Comput.-Aided Mol. Des.* **1990**, *4*, 1–105.
(24) Jorgensen, W. L.; Chandrasekhar, J.; Madura, J. D.; Impey, R. W.; Klein, M. L. *J. Chem. Phys.* **1983**, *79*, 926–935.
(25) Bianchi, A.; Bologni, L.; Dapporto, P.; Micheloni, M.; Paoletti, P. *Inorg. Chem.* **1984**, *23*, 1201–1205.
(26) Gran, G. *Analyst (London)* **1952**, *77*, 661–671.
(27) Gans, P.; Sabatini, A.; Vacca, A. *Talanta* **1996**, *43*, 1739–1753.
(28) Hall, J. P.; Izatt, R. M.; Christensen, J. J. *J. Phys. Chem.* **1963**, *67*, 2605–2608.
(29) Vacca, A. *AAAL program*, University of Florence: Florence, Italy, 1997.

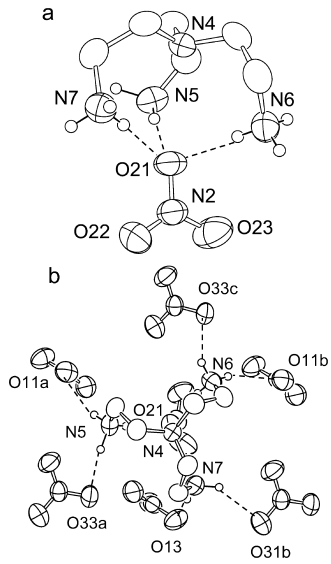

Figure 2. ORTEP drawing of (a) the $[H_3L(NO_3)]^{2+}$ anion adduct in the crystal structure of $[H_3L][NO_3]_3$ and (b) the same adduct surrounded by the H-bonded NO_3^- counterions.

Results and Discussion

Crystallographic Studies. The nitrate, $[H_3L][NO_3]_3$, and *p*-toluenesufonate, $[H_3L][TsO]_3$, adducts were obtained from the reaction of the free ligand with the corresponding acids in water. The crystal structure of $[H_3L][NO_3]_3$ contains $[H_3L(NO_3)]^{2+}$ adduct cations and nitrate anions. Figure 2a shows the ORTEP drawing of the adduct formed by a triprotonated H_3L^{3+} ligand and a firmly H-bonded nitrate anion. A selected list of H-bond contacts is reported in Table 2. The conformation assumed by the protonated ligand is featured by an overall noncrystallographic C_3 symmetry, the C_3 axis passing through the tertiary nitrogen. As shown in Figure 2, H_3L^{3+} forms a hemispherical cavity, of approximated 0.5 Å radius, where the O21 oxygen atom of the nitrate anion is partially hosted and forms three rather strong and linear hydrogen bonds (N···O distances ranging from 2.82 to 2.89 Å, Table 2) with the three protonated primary nitrogen atoms of H_3L^{3+}. As a consequence of this nitrate ion disposition, the $[H_3L(NO_3)]^{2+}$ adduct does not possess the C_3 noncrystallographic symmetry shown by the ligand.

Besides the contacts formed with O21, all protonated nitrogen atoms form two more H-bond interactions with external nitrate anions, giving rise to a dense H-bond network (Figure 2b). It is to be noted, however, that the interactions established with the external nitrates are generally weaker than those formed with O21 (Table 2).

The crystal structure of $[H_3L][TsO]_3$ consists of $[H_3L(TsO)]^{2+}$ adduct cations and TsO^- anions. The asymmetric unit contains two crystallographically independent adducts A and B (Figure 3). In A, the triprotonated H_3L^{3+} ligand displays two conformations slightly differing in the torsional angles of an ethylenic chain, which is +g in 60% and −g in 40% of the total population. An ORTEP drawing of the predominant conformer is depicted in Figure 3A. The overall conformation of H_3L^{3+} in both conformers, however, is quite similar and defines a hemispherical cavity, of approximated 0.5 Å radius, with a noncrystallographic C_3 symmetry analogous to that observed in the crystal structure of $[H_3L][NO_3]_3$. Also, the coordination features of the TsO^- anion in this adduct are quite similar to those found for NO_3^- in the previous structure, the *p*-toluensulfonate O11 oxygen being partially inserted into the ligand cavity, where it forms three rather strong H bonds (N···O distances ranging from 2.85 to 3.04 Å, Table 3) with the three protonated primary nitrogen atoms of H_3L^{3+}.

Also, adduct B is found in two equally populated conformations, which differ in the position of an ethylammonium chain. Actually, in one conformer (Figure 3B), the ligand assumes a conformation very similar to that found in the nitrate complex, but only two protonated primary nitrogens of H_3L^{3+} are involved in H bonds with an oxygen atom (O31) of the coordinated TsO^- anion (N7···O31, 2.83(1) Å; N8···O31, 2.82(1) Å; Table 3), the third ammonium group being located at a longer distance (N6′···O31, 3.46(3) Å; Table 3). The same coordination features are shown by the second conformer of adduct B (Figure 2B), in which the noninteracting ammonium group (N6) is located at a longer distance (N6···O31, 5.09(1) Å) and forms H-bond interactions with external TsO^- anions.

The tridentate binding mode is the most typical for H_3L^{3+} in crystal structures. It was also observed in the presence of other oxoanions, such as HPO_4^{2-},[30] $H_2PO_4^-$,[31] SO_4^{2-},[30] MoO_4^{2-},[32] ClO_4^-,[33] cyclohexaphosphate,[34] and halogenides[35] (Cl^-, Br^-, I^-). The same arrangement of H_3L^{3+} was also found with organic anions.[36] In particular, with 2-(2,6-dichlorophenyl)amino)phenyl)acetate,[36d] the ligand assumes both binding modes depicted in Figure 3 for TsO^-. On the other hand, a completely planar conformation of H_3L^{3+} is shown by the crystal structures of H_3LBr_3 and H_3LI_3.[37]

Binding Studies. Speciation of the adduct species was carried out by computer analysis of potentiometric (pH-metric) titration data performed by means of the HYPERQUAD[27] program, which furnished the corresponding overall equilibrium constants according to the general reaction

$$A^{n-} + L + mH^+ = [H_mL(A)]^{(m-n)+}$$

The overall equilibrium constants do not furnish any information about the location of H^+ ions in the adducts. Protonation of NO_3^-, SO_4^{2-}, and TsO^-, however, takes place only in very acidic solutions, well below the pH range used to perform the present study, and consequently the acidic protons in the adducts of these anions must be located on

(30) Ilioudis, C. A.; Georganopoulou, D. G.; Steed, J. W. *CrystEngComm* **2002**, *4*, 26–36.
(31) (a) Oueslati, J.; Rayes, A.; Nasr, C. B.; Lefebvre, F. *Phosphorus, Sulfur, Silicon, Relat. Elem.* **2006**, *181*, 693. (b) Dakhlaoui, A.; Smiri, L. S.; Driss, A. *Acta Crystallogr., Sect. E* , *60*, o2241.
(32) Alyea, E. C.; Ferguson, G.; Xu, Z. *Acta Crystallogr., Sect. C* **1995**, *51*, 353–356.
(33) Burgess, J.; Al-Alousy, A.; Fawcett, J.; Russell, D. R. *Acta Crystallogr., Sect. C* **1991**, *47*, 2506–2508.
(34) Marouani, H.; Rzaigui, M. *Solid State Sci.* **1999**, *1*, 395–408.
(35) (a) Rasmussen, S. E.; Gronbaek, R. *Acta Chem. Scand.* **1963**, *17*, 832–842. (b) Hazell, R. G.; Rasmussen, S. E. *Acta Chem. Scand.* **1968**, *22*, 348–350. (c) Ariyananda, W. G. P.; Norman, R. E. *Acta Crystallogr., Sect. E* , *59*, o160. (d) Kaminskii, A. A.; Bohaty, L.; Becker, P.; Held, P.; Eichler, H. J.; Rhee, H.; Hanuza, J.; Maczka, M. *Laser Phys. Lett.* **2006**, *3*, 490–494.

Table 2. Selected Bond Distances (Å) and Angles (deg) for the Hydrogen-Bond Contacts in the $[H_3L][NO_3]_3$ Crystal Structure

bond	distance	bond	distance	bonds	angle	symmetry relationship
N5···O21	2.854(4)	H51···O21	2.07(4)	N5−H51−O21	170(4)	
N6···O21	2.815(4)	H61···O21	1.99(4)	N6−H61−O21	170(4)	
N7···O21	2.885(4)	H73···O21	2.03(4)	N7−H73−O21	176(4)	
N5···O11a	2.867(4)	H52···O11a	2.08(5)	N5−H52−O11a	140(4)	$(-x+2, -y+1, -z+2)$
N5···O33a	3.063(4)	H53···O33a	2.03(5)	N5−H53−O33a	164(4)	$(-x+2, -y+1, -z+2)$
N6···O33c	2.894(5)	H63···O33c	2.10(5)	N6−H63−O33c	148(4)	$(-x+1.5, +y-0.5, -z+1.5)$
N6···O11b	3.021(5)	H62···O11b	2.27(5)	N6−H62−O11b	147(4)	$(-x+1, -y+1, -z+2)$
N7···O31b	3.226(4)	H71···O31b	2.41(5)	N7−H71−O31b	140(4)	$(-x+1, -y+1, -z+2)$
N7···O13	2.873(4)	H72···O13	2.01(5)	N7−H72−O13	163(4)	

Table 3. Bond Distances (Å) and Angles (deg) for the Selected Hydrogen Bond Contacts in the $[H_3L][TsO]_3$ Crystal Structure

bond(s)	distance/angle	symmetry relationship
N2···O11	2.85(1)	
N3···O11	2.91(1)	
N4···O11	3.040(9)	
N7···O31	2.83(1)	
N8···O31	2.82(1)	
N7···O62	3.26(1)	
N7···O43	2.83(1)	
N4···O23	2.83(1)	
N4···O61	2.89(1)	
N3···O52	3.10(1)	
N3···O53	3.32(1)	
N2···O13a	2.852(8)	$(-x+2, -y+1, -z+1)$
N4···O12a	2.87(1)	$(-x+2, -y+1, -z+1)$
N6′···O32b	3.18(3)	$(-x+1, -y, -z+2)$
N6···O42b	2.81(2)	$(-x+1, -y, -z+2)$
N6···O32b	2.89(1)	$(-x+1, -y, -z+2)$
N6′···O42b	3.33(3)	$(-x+1, -y, -z+2)$
N8···O52c	3.34(1)	$(x-1, y, z)$
N8···O51c	2.87(1)	$(x-1, y, z)$
N8···O21d	2.926(9)	$(-x+1, -y+1, -z+1)$

the ligand. On the other hand, the phosphate-type anions undergo multiple protonations over a wide pH range. In this case, the proton location in the adducts was assumed to be regulated by the basicity of the interacting species. The

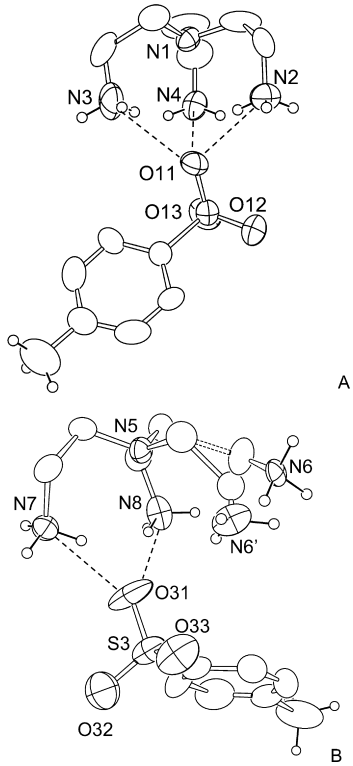

Figure 3. ORTEP drawings of A and B conformers of the $[H_3L(TsO)]^{2+}$ anion adduct in the crystal structure of $[H_3L][TsO]_3$.

Table 4. Stability Constants and $\Delta H°$ and $T\Delta S°$ Values of Anion Adducts Determined in 0.10 M NMe_4Cl Aqueous Solutions at 298.1 ± 0.1 K[a]

equilibria	log K	$\Delta H°$ (kJ/mol)	$T\Delta S°$ (kJ/mol)
$HL^+ + NO_3^- = [HL(NO_3)]$	2.71(9)	2.85(4)	18.3(4)
$H_2L^{2+} + NO_3^- = [H_2L(NO_3)]^+$	3.02(8)	0.8(3)	18.0(4)
$H_3L^{3+} + NO_3^- = [H_3L(NO_3)]^{2+}$	3.45(9)	1.8(3)	21.5(4)
$HL^+ + SO_4^{2-} = [HL(SO_4)]^-$	1.66(8)	−5.0(3)	4.5(4)
$H_2L^{2+} + SO_4^{2-} = [H_2L(SO_4)]$	1.72(4)	−2.3(3)	7.5(4)
$H_3L^{3+} + SO_4^{2-} = [H_3L(SO_4)]^+$	2.22(2)	−3.0(2)	9.7(2)
$HL^+ + TsO^- = [HL(TsO)]$	1.56(8)	−7.5(4)	1.40(4)
$H_2L^{2+} + TsO^- = [H_2L(TsO)]^+$	1.46(7)	−22.6(4)	−14.3(4)
$H_3L^{3+} + TsO^- = [H_3L(TsO)]^{2+}$	1.78(4)	−25.9(4)	−15.7(4)
$H_2L^{2+} + HPO_4^{2-} = [H_2L(HPO_4)]$	1.89(5)	−20.1(4)	−9.3(4)
$H_3L^{3+} + HPO_4^{2-} = [H_3L(HPO_4)]^+$	2.66(1)	−9.0(3)	6.2(3)
$H_2L^{2+} + P_2O_7^{4-} = [H_2L(P_2O_7)]^{2-}$	3.70(9)	−5.0(4)	16.1(4)
$H_3L^{3+} + P_2O_7^{4-} = [H_3L(P_2O_7)]^-$	5.78(2)	−8.3(4)	24.7(4)
$H_3L^{3+} + HP_2O_7^{3-} = [H_3L(HP_2O_7)]$	3.90(9)	−5.2(4)	17.0(4)
$H_2L^{2+} + P_3O_{10}^{5-} = [H_2L(P_3O_{10})]^{3-}$	4.42(9)	−6.7(4)	18.5(4)
$H_3L^{3+} + P_3O_{10}^{5-} = [H_3L(P_3O_{10})]^{2-}$	6.70(3)	−9.8(2)	28.4(2)
$H_3L^{3+} + HP_3O_{10}^{4-} = [H_3L(HP_3O_{10})]^-$	4.74(3)	1.1(2)	28.1(2)
$H_3L^{3+} + H_2P_3O_{10}^{3-} = [H_3L(H_2P_3O_{10})]$	3.69(5)	28.6(2)	49.7(2)

[a] Values in parentheses are standard deviations on the last significant figures.

stability constants listed in Table 4 were calculated according to these roles.

The general procedure for determining equilibrium constants, involving ionic species in solution, requires the use of an inert electrolyte, in high concentration with respect to reactants and products, to keep constant the ionic strength during the measurements. In the case of anion binding equilibria, however, it is highly improbable that the so-called inert electrolyte can be really innocent, since its anionic part can compete with the anion under consideration. Accordingly, we expect that some interaction of the protonated forms of L takes place with Cl^- anions coming from the electrolyte we used in our measurements, under the experimental conditions employed ($[Me_4NCl] = 0.10$ M). Nevertheless, the analysis of titration data revealed unambiguously the formation of L adducts with the studied anions, leading to the determination of the relevant stability constants (Table 4).

As far as the stoichiometry of the species formed is considered (Table 4), it is to be noted that, despite the different charge, size, molecular architecture, and number of the binding groups in the anions, only adducts with 1:1

(36) (a) Glidewell, C.; Ferguson, G.; Gregson, R. M.; Campana, C. F. *Acta Crystallogr., Sect.B* **2000**, *56*, 68. (b) Lynch, D. E. *Acta Crystallogr., Sect. E* , *59*, o1076. (c) Lynch, D. E. *Acta Crystallogr., Sect. E* , *59*, o115. (d) Lynch, D. E.; Bening, A. S.; Parsons, S. *Acta Crystallogr., Sect. E* , *59*, o131.

(37) Ilioudis, C. A.; Hancock, K. S. B.; Georganopoulou, D. G.; Steed, J. W. *New J. Chem.* **2000**, *24*, 787–798.

anion/receptor stoichiometry were found in solution. This is a common features of anion adducts, which need many binding contacts between the interacting partners to reach significant stability. Preorganized receptors, like L, which offers a tripodal conformation of convergent binding groups to the anionic substrates, are particularly favored in this respect, since they do not have to spend energy to acquire the appropriate conformation and, furthermore, they are structured to direct their binding action toward a single anion. Accordingly, protonated forms of L are able to bind even monocharged anions, such as NO_3^- and TsO^-, in a solvent with a high dielectric constant like water.

As can be seen from Table 4, for a given anion, the adduct stability increases with increasing charge of the interacting partners, in agreement with an essentially electrostatic nature of the interaction, although, hydrogen bonding is also expected to favorably contribute to the formation of these species, in particular with phosphate-type anions, which are good acceptors and donors of hydrogen bonds. The stability of these adducts well compares with the stability of analogous species with polyammonium macrocycles,[38,39] confirming that L is among the most preorganized receptors for anion binding. In particular, it is interesting to note that the stability constant for the binding of nitrate by the tricharged H_3L^{3+} species (log K = 3.45(9), Table 4) is comparable with the highest stability constant (log K = 3.11(5),[8c] 3.73(6)[9f]) reported for the caged nitrate complex with the hexacharged form of the macrobicyclic receptor L1, which hosts the anion in a three-dimensional cavity based on the L structure. This occurs despite the greater charge of the last receptor and the experimental occurrence that the relevant constant was determined in the presence of 0.1 M TsO^-, which is a lesser competing medium,[8c,9f] in particular for small cagelike ligands, than the 0.1 M Cl^- solution we adopted for the determination of our stability constants. Taking into account that bicyclic ligand cavities are less solvated (more favored) than open ligands, it seems reasonable to ascribe the high stability of the nitrate adduct with L to a greater adaptability of this ligand toward the anion. As a matter of fact, also for tren-based bicyclic receptors, ligand adaptability to the hosted anions appears to be of great importance, to such an extent that nitrate encryption may become an unfavorable process.[15]

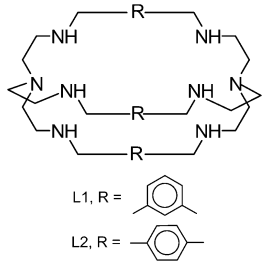

The crystal structure of H_6L1^{6+} containing two nitrates[8e,9f] showed that the anions are bound to the H_3L^{3+}-like units perpendicularly to the C_3 axis passing through the tertiary nitrogen atom, in contrast to the binding mode assumed by nitrate in the crystal structure of $[H_3L(NO_3)]^{2+}$. However, in the crystal structure[6c] with the hexaprotonated form of the similar macrobicycle L2, a single nitrate anion is bound into the ligand cavity, featuring the arrangement observed for $[H_3L(NO_3)]^{2+}$. In this case, the two nitrate oxygens not involved in hydrogen bonds with the triprotonated tripodal unit are hydrogen bound to two water molecules located outside the cavity, in the ligand clefts, and firmly anchored to the ammonium groups of the second triprotonated tripodal unit. The different binding features shown by this anion in the three crystal structures raised the question of nitrate arrangement in the $[H_3L(NO_3)]^{2+}$ adduct in solution. Since, for similar systems, in which the substrate is weakly bound by the receptor and is rapidly exchanged with the free species, direct experiments, such as spectroscopic measurements, are not able to give information about this issue, we performed a modeling study on $[H_3L(NO_3)]^{2+}$, considering both nitrate binding modes (*a* and *b* in Figure 1). Calculations performed in the gas phase showed that *b* is the most stable conformation with an energy gap of about 40 kJ/mol. Nevertheless, when solvent effects were taken into account by using the Poisson−Boltzmann method[20] (see Experimental Section), the energy difference between the two conformations decreases significantly to about 8 kJ/mol. These results suggest that the binding mode *a* observed in the crystal structure is not only determined by the interactions in the solid state but may reflect the situation in solution. Preliminary calculations performed to evaluate the energy difference between the two conformations were also carried out by using the empirical force field AMBER3[21] and the TIP3P model[24] of water molecules, to explicitly take into account solvation effects. After one cycle of the simulated annealing procedure, conformation *a* was found to be more stable than *b*. According to these modeling calculations, we expect that the main conformation adopted by $[H_3L(NO_3)]^{2+}$ in solution is similar to that observed in the crystal structure, although the simultaneous presence of adducts with the *b* conformation, at least as minor species, cannot be excluded.

The C_3 symmetry of nitrate can be recognized in the other anions studied in this works, and then nitrate can be used as a model for their interaction with protonated forms of L. Indeed, it is worth noting that binding mode *a* was also found in the crystal structure of the TsO^- adduct described above, even when the receptors involved only two protonated amine groups to bind TsO^-.

In contrast to nitrate binding, sulfate binding is favored by the cagelike structure of L1. The stability constant determined in a 0.10 M Cl^- solution, which allows a strict comparison with our value, for SO_4^{2-} binding by H_6L1^{6+} (log K = 4.43(1)),[8c] is significantly higher than that which we found for the sulfate adduct with H_3L^{3+} (log K = 2.22(2), Table 4). In this case, the large anion can interact with both binding units of L1, giving rise to a greater number of charge−charge and hydrogen-bonding interactions, which stabilize the complex, as shown in the solid state by crystal structures of some tetrahedral oxoanions caged into H_6L1^{6+}.[6d]

Further comparisons are not possible since, to our knowledge, no stability constants for adduct formation in aqueous solution by L1, or other pertinent tren derivatives, with the remaining anions analyzed in this work have been reported.

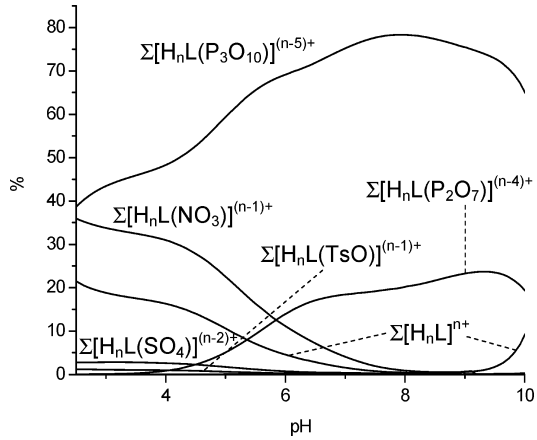

Figure 4. Selectivity diagram calculated for the system $L/NO_3^-/ SO_4^{2-}/ TsO^-/ PO_4^{3-}/ P_2O_7^{4-}/ P_3O_{10}^{5-}$ showing the percentage of the overall concentration of receptors bound to each anion, in the presence of all anions, as a function of pH. All reagents 1×10^{-3} M.

Another interesting issue is the selectivity of tren in anion binding. For this type of system, in which both the receptor and anions can be involved in multiple protonation equilibria, the straightforward comparison of stability constants is generally an improper approach to analyzing selectivity. A useful computational method[40] balancing all complex stability constants along with receptors' and substrates' basicity can be used to calculate the percentage of the species formed, as a function of pH, in a competitive system containing equimolar amounts of the receptor and all anions and to plot the overall percentages of the adducts formed by the competing reactants versus pH. This criterion allows for attributing selectivity over the pH range. When the formation of adducts different from those found in the noncompetitive systems is reasonably improbable, like in the case of tren, which shows a marked tendency to form only 1:1 adducts, this method furnishes confident results. A selectivity diagram obtained by this method is reported in Figure 4. As can be seen, tren shows an evident binding selectivity toward triphosphate over the studied pH range. In particular, in neutral and fairly alkaline solutions, adducts of triphosphate are formed up to 80%, around pH 8, the remaining 20% being almost exclusively constituted by diphosphate adducts. Such behavior can be ascribed to the strong electrostatic interaction occurring in this pH region between the positively charged receptor and these highly charged anions. At higher pH, the formation of adducts vanishes with the positive charge on the receptor. On the other side, when the solution becomes increasingly acidic, the negative charge on these anions is reduced by protonation, and their ability to interact with the receptor decreases as well. It is noteworthy that, under these conditions, nitrate adducts become abundant species, evidencing a marked ability of tren in recognizing nitrate over all of the other anions but triphosphate. As a matter of fact, calculations performed in absence of triphosphate, for a solution containing tren and all of the other anions in millimolar concentrations, show that at pH 3, for instance, 52% of the receptos are involved in the formation of nitrate adducts while only 2.5% are bound to the remaining anions.

Enthalpic and Entropic Contributions. To get more insight into the nature of the interaction processes studied in this work, we measured the enthalpy changes associated with the binding of anions by the protonated forms of L. The values obtained are listed in Table 4 along with the derived entropy changes.

According to a simple electrostatic model, the formation of ion pairs between rigid cations and anions (hard sphere with embedded point charges) in an ideal structureless homogeneous solvent is expected to be accompanied by slightly unfavorable $\Delta H°$ contributions and largely favorable entropic terms, principally deriving from the desolvation of the interacting species brought about by charge neutralization occurring in the pairing process.[3b]

The values reported in Table 4 show that, with few exceptions, the binding of the considered anionic substrates is promoted by favorable entropic changes, while the enthalpic ones are almost negligible or slightly favorable, in fairly good agreement with the expectations based on the electrostatic model. Accordingly, desolvation processes appear to give a determinant contribution to the formation of these anion adducts. An evident exception to this role is observed for the binding of the TsO^- anion. Due to the presence of the aromatic residue connected to the anionic part of TsO^-, the oxygen atoms involved in the interaction with the ammonium receptor are less solvated, with respect to the other anions. Accordingly, a lower desolvation is expected upon the interaction of TsO^- with the positively charged receptor, leading to a more favorable enthalpic effect and a lower entropic gain, in agreement with the results obtained for this anion (Table 4). The loss of freedom experienced by the receptor and substrate upon interaction makes the binding process entropically unfavorable. As a matter of fact, the higher the charge on the receptor, the higher the entropy loss (Table 4), since more freedom is lost upon stronger association.

Another exception to the above role is given by HPO_4^{2-}. This anion interacts with H_2L^{2+}, giving rise to a largely favorable and predominant enthalpic contribution, while the entropic one is unfavorable. A distinctive binding feature that may occur only for $[H_2L(HPO_4)]$, among all adducts under consideration, is the formation between the interacting partners of hydrogen bonds of types 1 and 2 (schemes below), involving a primary unprotonated amine group and a protonated oxygen atom of phosphate.

$$-N|\cdots H-O- \quad (1)$$

$$-N-H\cdots OH- \quad (2)$$

It is known that type 2 hydrogen bonds are largely weaker than type 1 ones, which give the major contribution.[38] Taking

(38) (a) Jeffrey, G. A. *An Introduction to Hydrogen Bonding*; Oxford University Press: New York, 1997. (b) Bazzicalupi, C.; Bencini, A.; Bianchi, A.; Cecchi, M.; Escuder, B.; Fusi, V.; Garcia-España, E.; Giorgi, C.; Luis, S. V.; Maccagni, G.; Marcelino, V.; Paoletti, P.; Valtancoli, B. *J. Am. Chem. Soc.* **1999**, *121*, 6807–6815.
(39) Arranz, P.; Bencini, A.; Bianchi, A.; Diaz, P.; Garcia-España, E.; Giorgi, C.; Luis, S. V.; Querol, M.; Valtancoli, B. *J. Chem. Soc., Perkin Trans. 2* **2001**, 1765–1770.
(40) Bianchi, A.; Garcia-España, E. *J. Chem. Educ.* **1999**, *76*, 1727–1732.

into account that protonation of the L amine group is a strongly exothermic reaction while deprotonation of the HPO_4^{2-} is fairly endothermic (Table S1, Supporting Information), the partial anion-to-amine proton transfer processes involved in hydrogen bonding mode 1 are expected to give a significantly favorable enthalpic contribution to the formation of $[H_2L(HPO_4)]$, in agreement with the enthalpy change observed to accompany its formation (Table 4). On the other hand, this type of interaction, involving two uncharged groups, produces some charge separation due to the partial proton transfer occurring between the two groups, and accordingly, it is expected to favor a stronger solvation accompanied by an unfavorable entropic effect, as actually found for $[H_2L(HPO_4)]$ (Table 4). This means that the binding of HPO_4^{2-} with H_2L^{2+} would involve two oxygen atoms of the anion, instead of one as observed in the crystal structures of the NO_3^- and TsO^- adducts with H_3L^{3+}. In the TsO^- complex, however, the H_3L^{3+} receptor adopts two binding modes, one of which involves only two protonated amine groups in the binding, the third one remaining unbound in relatively close proximity to the anion. It seems quite reasonable to assume that this unbound ammonium group is that giving rise to the free primary amine group in the complexes of H_2L^{2+}. According to this model, this unprotonated amine group would be available for the formation of a type 1 hydrogen bonds with HPO_4^{2-} in the $[H_2L(HPO_4)]$ complex, the two protonated amine groups of H_2L^{2+} being involved in the chelation of a deprotonated phosphate oxygen, as schematically represented in Figure 5.

Figure 5. Schematic representation of the interaction mode in $[H_2L(HPO_4)]$.

Conclusions

The tripodal ligand tren has been largely used as a building block and binding unit for the preparation of C_3-symmetry macrobicyclic anion receptors able to encrypt within the receptor cavity anionic substrates of different types, in particular oxoanions having the same C_3 symmetry. In spite of the large interest for tren as a component of such receptors, no information on the anion binding properties of the isolated tren molecules in solution was reported until now.

The present study performed in aqueous solution shows that association of the protonated forms of L with oxoanions such as NO_3^-, SO_4^{2-}, TsO^-, PO_4^{3-}, $P_2O_7^{4-}$, and $P_3O_{10}^{5-}$ does take place, in spite of the noninnocent character of this solvent, highly capable of hydrogen-bonding and dipole interactions. The adduct stability is mostly determined by favorable entropic contributions deriving from desolvation occurring upon charge neutralization of the interacting partners, the enthalpy contributions being generally negligible or fairly favorable.

The anion binding modes of L can be different from those found for cagelike receptors based on L units, as observed in crystal structures, and solvent interactions play an active role in determining the anion−receptor arrangement. Nevertheless, L appears to be a good receptor even in a low protonation state, owing to its tripodal preorganization, enabling the formation of many charge−charge and hydrogen-bond contacts with the anions.

In conclusion, the use of tren as a building block for the assembly of anion receptors is a striking choice, not only for its preoganized structure with C_3 symmetry, which facilitates the synthesis of cagelike receptors and promotes topological matching with anions of the same symmetry, but also thanks to its intrinsic ability to bind anions, even in water.

Supporting Information Available: Table of equilibrium constants; $\Delta H°$ and $T\Delta S°$ values for protonation of tren, phosphate, diphosphate, and triphosphate anions; and crystallographic information files (CIF) for $[H_3L][NO_3]_3$ and $[H_3L][TsO]_3$. This material is available free of charge via the Internet at http://pubs.acs.org.

IC8013128